Near-yrast structure of odd-A, neutron-rich Pr isotopes

T. Malkiewicz, G. S. Simpson, W. Urban, J. Genevey, U. Köster, T. Materna, J. A. Pinston, M. Ramdhane, T. Rząca-Urban, G. Thiamova, A. G. Smith, I. Ahmad, and J. P. Greene

Phys. Rev. C **85**, 044314 — Published 16 April 2012

DOI: 10.1103/PhysRevC.85.044314

Near-yrast structure of odd-A, neutron-rich Pr isotopes

T. Malkiewicz,[1] G. S. Simpson,[1,*] W. Urban,[2,3] J. Genevey,[1] U. Köster,[2] T. Materna,[2] J. A. Pinston,[1] M. Ramdhane,[1] T. Rząca-Urban,[3] G. Thiamova,[1] A. G. Smith,[4] I. Ahmad,[5] and J. P. Greene[5]

[1] *LPSC, Université Joseph Fourier Grenoble 1, CNRS/IN2P3, Institut National Polytechnique de Grenoble, F-38026 Grenoble Cedex, France*

[2] *Institut Laue-Langevin, B.P. 156, F-38042 Grenoble Cedex 9, France*

[3] *Faculty of Physics, University of Warsaw, ul.Hoża 69, PL-00-681 Warszawa, Poland*

[4] *Department of Physics and Astronomy, The University of Manchester, M13 9PL Manchester, UK*

[5] *Argonne National Laboratory, Argonne, Illinois 60439, USA*

(Dated: March 26, 2012)

The neutron-rich praseodymium isotopes ^{151}Pr and ^{153}Pr have been studied by prompt γ-ray spectroscopy using ^{248}Cm and ^{252}Cf spontaneous-fission sources placed inside the EUROGAM-II and Gammasphere germanium arrays, respectively. Rotational bands, based on $3/2^-[541]$ states, with similar structures, have been assigned to these nuclei. These bands decay by intraband $E2$ transitions. Interband $E1$ transitions, reported in other works, were not observed. Delayed conversion-electron and γ-ray spectroscopy of an $A = 151$ nucleus has been performed at the Lohengrin mass spectrometer. A previously reported 35.1-keV isomer of ^{151}Pr has been determined to decay by an $E1$ transition and its half-life of 50(8) μs measured for the first time. Calculations performed using a reflection-symmetric quasi-particle-rotor model successfully reproduce the energies of the excited states of these nuclei and their decay patterns. The spin of the isomer has been assigned to be $(1/2^+, 3/2^+)$ from a comparison with the calculations. The long half life of this isomer and the lack of intraband $E1$ transitions show an absence of strong octupole correlations in the observed states of ^{151,153}Pr. This is explained in terms of increasing quadrupole deformation reducing the number of Nilsson orbitals close to the Fermi surface available to form octupole collectivity.

PACS numbers: 23.35.+g, 23.20.Lv, 27.70.+q, 21.10.Tg, 25.85.Ec, 25.85.Ca

I. INTRODUCTION

The presence of strong octupole correlations in the neutron-rich lanthanide nuclei is a well established phenomenon [1–3]. These correlations are generated by two pairs of so-called $\Delta I = \Delta l = 3$ orbitals which lie close to the Fermi surface here and allow $\pi(h_{11/2}, d_{5/2})_{3^-}$ and $\nu(i_{13/2}, f_{7/2})_{3^-}$ octupole couplings, leading to the appearance of strong octupole modes in ^{144}Ba [2, 4] for example. Despite numerous studies in this region, our knowledge on this subject is far from complete. For example, it is not yet clear how the octupole couplings here are affected by the strong static quadrupole deformation, which suddenly appears beyond neutron number $N = 90$ [5], and how far the softness to octupole modes extends.

An interesting possibility is that in odd-A nuclei octupole correlations are reduced. We have observed the latter effect in three odd-A Cs isotopes [6] and recently in ^{149}Pr [7]. It is interesting to study more Pr isotopes, especially at higher neutron number, to verify this observation as well as to follow the evolution of octupole correlations with increasing neutron number and quadrupole deformation. This is even more urgent now, after a recent claim of well developed octupole bands in ^{151}Pr and ^{153}Pr [8, 9], a situation which differs significantly from that reported for the neighboring nucleus ^{149}Pr [6].

* simpson@lpsc.in2p3.fr

Proper isotopic identification is paramount when studying fission fragments. Our work on ^{149}Pr has been facilitated by a measurement of isomeric states of Rb nuclei, populated following the cold-neutron induced fission of ^{235}U at the ILL Grenoble [10, 11]. This unique identification of several Rb isotopes paved the way to study the Pr isotopes produced, as the Rb and Pr isotopes are complementary fragments in the spontaneous fission of ^{248}Cm. From the fission of ^{248}Cm we have a rich data set of triple-γ coincidences. Studies of complementary fission fragments rely on the mass identification procedure first proposed by Hotchkis *et al.* [12]. The quality of this method is illustrated in Fig. 2 (upper panel) of Ref. [13], one of a few dozens of publications, where this method has been applied to date. For example, in Ref. [13] an exotic ^{139}Te nucleus, which is very weakly produced in spontaneous fission of ^{248}Cm, has been identified in this way. In addition, the production level of a given isotope can be used to support its identification as illustrated in the lower panel of Fig. 2 in Ref.[13].

It is our experience that the identification of the odd-Z isotopes in a set of high-fold γ coincidence data is more difficult than even-Z nuclei, probably due to the higher fragmentation of collective bands in odd-Z nuclei. This sometimes leads to assignment inaccuracies when relying only on prompt-fission coincidences, as illustrated by a complex history of the identification of the Pr isotopes in previous works. The excitation scheme first proposed for the isotope ^{147}Pr [14, 15] has been later assigned to ^{144}La [16]. The excitation scheme of ^{149}Pr proposed in [17] has been replaced by another scheme [14, 15]. We have confirmed this scheme, but changed the spin assignments and the interpretation [7]. The nucleus ^{151}Pr, which is studied in this work has been assigned a level scheme first in [14, 15], which was previously assigned to ^{149}Pr [17]. However, recently the excitation scheme of ^{151}Pr has been changed entirely [8, 9]. The previous scheme of ^{149}Pr, proposed in [17], has now been assigned to ^{150}Pr [8, 9], in agreement with the mass assigments shown later in Sec. II B.

The purpose of this work, is to provide independent data and isotopic identification for decays of ^{151}Pr and ^{153}Pr nuclei reported recently from fission of ^{252}Cf [8, 9]. This has been performed by measurements of prompt γ rays following the spontaneous fission of ^{248}Cm and ^{252}Cf sources. In particular we would like to verify the presence of parity-doublet bands in both nuclei, claimed in Ref. [8]. Such bands would not agree with our conclusions about the level of octupole effects in odd-Z nuclei [6] and in nuclei with $N > 92$ [18, 19]. A 35.1-keV isomeric state of ^{151}Pr has been reported [20] and so delayed γ-ray and conversion-electron spectroscopy of mass 151 nuclei has also been performed to give a more complete picture of the structure of this nucleus.

II. EXPERIMENTS AND RESULTS

In the present work we have searched for μs isomeric states in the neutron-rich Pr isotopes using the Lohengrin mass spectrometer of the Institut Laue-Langevin, Grenoble. Furthermore, we have used high-fold, γ-ray coincidence data collected with EUROGAM-II and Gammasphere arrays of escape-suppressed germanium detectors to search for medium-spin excitations in these nuclei. We have also used our set of data from the spontaneous fission of ^{252}Cf, collected with Gammasphere, to verify our results from the fission of ^{248}Cm. A detailed description of these measurements and the results obtained follows.

A. Lohengrin measurement

Delayed transitions in a neutron-rich $A = 151$ nucleus were studied using the Lohengrin mass spectrometer of the high-flux reactor of the Institut Laue-Langevin, Grenoble. These nuclei were produced using an 0.87 mg/cm^2, 7×0.5 cm^2, ^{241}Am target, which mostly fissioned following two successive thermal-neutron captures. The $A = 151$ fission fragments had a flight time of around 2.7 μs through the spectrometer and were identified by a split-anode ΔE_1–ΔE_2 ionization chamber. Delayed γ rays and conversion electrons were detected by two Clover Ge detectors and a segmented Si(Li)detector, respectively. Events were recorded on disk up to 40 μs after the arrival of an $A = 151$ ion. The experimental setup is identical to that described in detail in Ref. [18] and both experiments ran during the same beam-time.

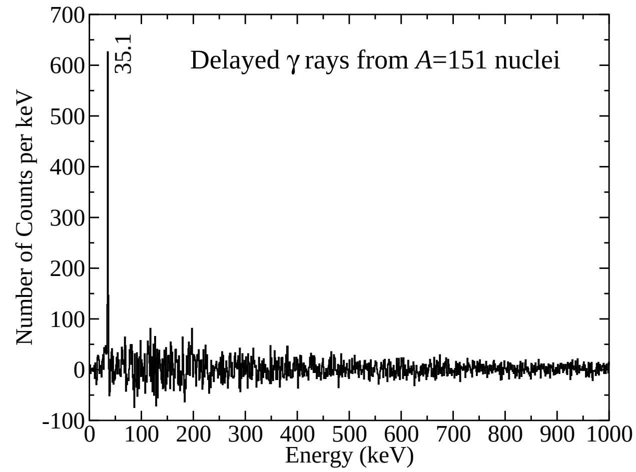

FIG. 1. Background-subtracted spectrum of delayed γ rays, detected by the Ge detectors at Lohengrin up to 15 μs after the arrival of an $A = 151$ ion.

Figure 1 shows background-subtracted delayed, γ rays measured in the Ge detectors up to 15 μs after the arrival of an $A = 151$ ion. The γ-ray background was obtained from ion-γ events recorded in a 15-μs period towards the end of the ion-γ coincidence window. A peak can clearly be seen in Fig. 1 at 35.1(2) keV, in agreement with the results reported i n [20]. This isomeric state was assigned to an excited state of ^{151}Pr in [20], based on the β-decay half life of its parent.

Background-subtracted delayed conversion-electrons and γ rays measured in the Si(Li) detectors up to 15 μs after the arrival of an $A = 151$ ion, are shown in Fig. 2. The background was selected in an identical way to that described above for the Ge-detector spectrum. A comparison of electron and γ-ray peak areas in Fig. 2 gives conversion coefficients of $\alpha_L = 0.6(2)$ and $\alpha_M = 0.11(4)$ for the 35.1-keV transition. Consistent results are also obtained if one uses the Ge-detector spectrum to obtain the absolute intensity of the 35.1-keV γ-ray [$\alpha_L = 0.8(3)$ and $\alpha_M = 0.14(5)$]. Combining these values gives a weighted mean of $\alpha_L = 0.66(17)$ and $\alpha_M = 0.12(3)$. These results are in excellent agreement with the expected values 0.587(9) and 0.124(2) respectively for an $E1$ transition [21]. The L and M conversion coefficients for an $M1$ transition [$\alpha_L = 3.24(5)$, $\alpha_M = 0.68(1)$], and higher multipolarities, are much larger and so can be ruled out. The 35.1-keV transition is therefore assigned as $E1$ in nature. Evidence of only one transition can be seen in both the delayed γ-ray and conversion-electron spectra and no other $\gamma - \gamma$, γ–X or $\gamma - e^-$ coincidences were observed, hence the energy of the isomeric state can be assigned to be at 35.1 keV.

By gating on the delayed 35.1-keV γ ray, and fitting the exponential decay shown in Fig. 3 a half life of 50(8) μs was determined. This corresponds to a reduced transition rate of $B(E1) = 6.3(10) \times 10^{-8}$ W.u. (Weisskopf units).

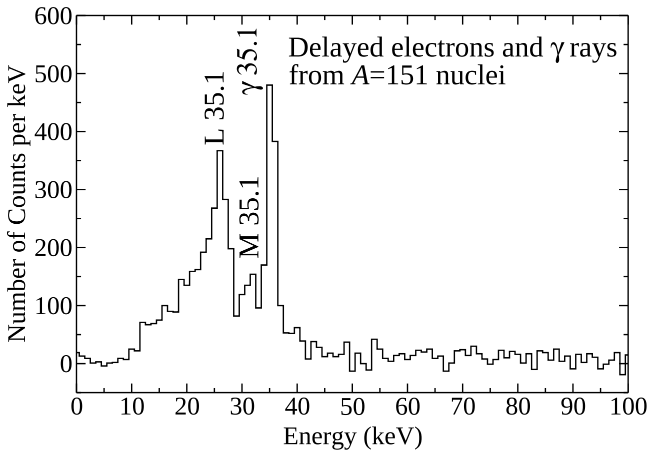

FIG. 2. Background-subtracted, delayed conversion-electrons and γ rays observed up to 15 μs after the arrival of an $A = 151$ ion in the Si(Li) detectors.

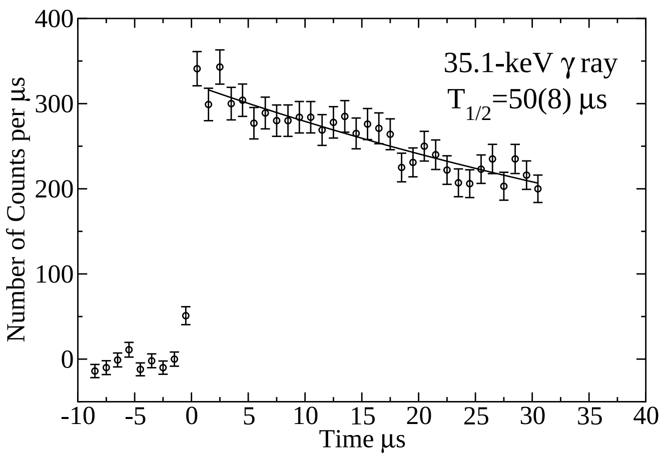

FIG. 3. Time spectrum of 35.1-keV γ rays in coincidence with $A = 151$ ions.

Using this half life, the total number of isomeric nuclei produced could be obtained. The mass 151 nuclei strongly produced in the double-neutron capture fission of ^{241}Am are distributed as follows, 5.0(31), 57.7(278), 35.2(125), and 2.0(12) % for ^{151}Ce, ^{151}Pr, ^{151}Nd, and ^{151}Pm, respectively [22]. From the total number of $A = 151$ nuclei detected in the chamber and the isobaric percentages above, an isomeric ratio $N(^{151}Pr_{isomer})/N(^{151}Pr_{total})$ of 19(12) % was determined for the 35.1-keV state of ^{151}Pr. By calculating other possible isomeric ratios, it can also be shown that the 35.1-keV isomer can only be an excited state in ^{151}Pr or ^{151}Nd, as this value would be greater than 100 % for the other $A = 151$ nuclei produced in this fission reaction. As the low-lying excited states of ^{151}Nd have been well studied, using a variety of reactions [23], then this gives an independent verification of the assignment of the 35.1-keV isomer to ^{151}Pr.

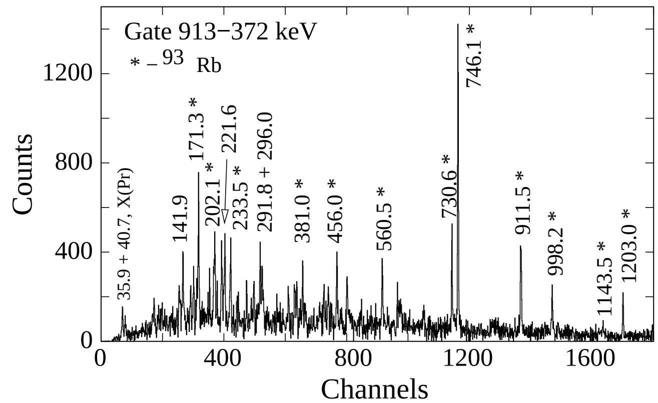

FIG. 4. A γ-ray spectrum obtained by double gating on transitions of ^{93}Rb. New lines are observed at 141.9-, 221.6-, 291.8 and 296.0-keV.

B. EUROGAM-II Measurement

A measurement of γ rays emitted following the spontaneous fission of a ^{248}Cm source, performed using the EUROGAM-II array of escape-suppressed germanium detectors [24] has provided $2{\times}10^{10}$ triple γ coincidence events. This data set has allowed searches for very weakly populated fission products [25]. We have already reported the observation of prompt γ decays from ^{149}Pr [6] from this data set. The maximum population of the Pr isotopes is expected at around mass $A = 151$ [22], therefore this data set should also contain γ decays of both ^{151}Pr and ^{153}Pr. The EUROGAM-II array was additionally equipped with four Low-Energy Photon Spectrometers (LEPS), which allowed the measurement of X rays and low-energy γ rays. Any detected X rays can be used to verify proton number assignments as well as to estimate conversion-electron coefficients. Furthermore, due to the range of angles between the germanium detectors of EUROGAM-II, angular correlations between γ rays in a cascade could be determined (more details on this technique can be found in previous publications [4, 26]).

The nucleus ^{93}Rb is expected to be the most likely fission partner of ^{151}Pr, hence double gates were set on the 913–372-keV prompt transitions of this nucleus [11], producing the spectrum shown in Fig. 4. New lines of energy 141.9, 221.6, 291.8, and 296.0 keV are visible in this spectrum and as they do not belong to the known decay scheme of ^{93}Rb they must belong to a Pr nucleus.

Gating on the 913-keV line of ^{93}Rb and the new 221.6-keV line revealed the spectrum shown in Fig. 5, where further new lines are present, with the two strongest seen at 291.8 and 296.0 keV.

In Figs. 6(a) and (b) γ-ray spectra are shown which were made by setting a double gate on the 221.0- and 291.8-keV and on the 221.8- and 296.0-keV lines, respectively. It is clear that *two* new different cascades are observed, though with rather similar γ-ray transition ener-

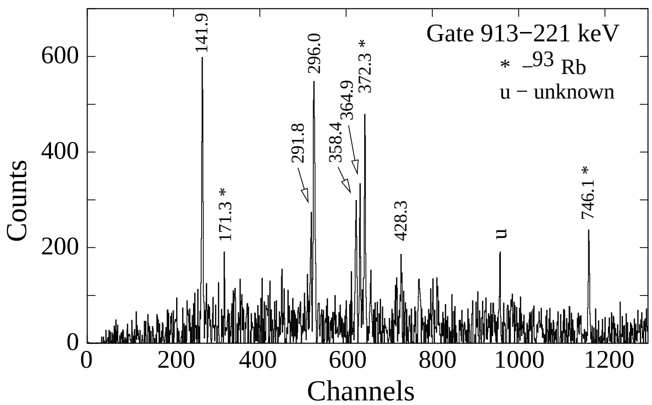

FIG. 5. A γ-ray spectrum double-gated on the 913-keV line of ^{93}Rb and the new 221.6-keV line.

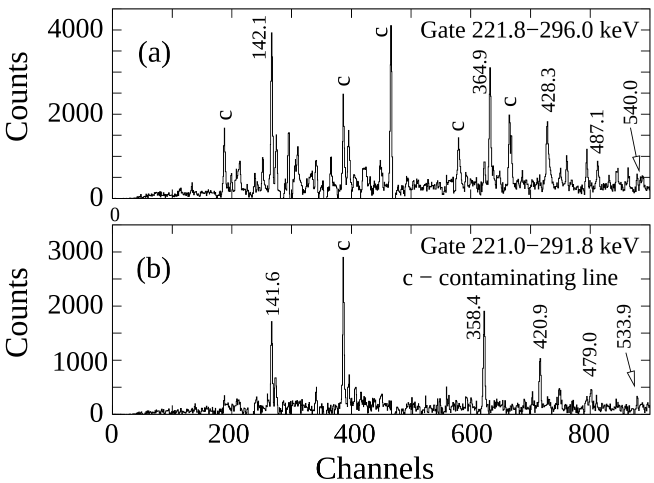

FIG. 6. Two γ-ray spectra obtained by double-gating on a) the 221.8- and 296.0-keV lines and b) the 221.0- and 291.8-keV lines of the new cascades.

gies. The multipolarities of the most intense transitions in these cascades can be assigned to be $E2$–$E2$, from the angular correlation measurements shown in Fig. 7. From the relative intensities of the transitions in these cascades the decay schemes shown in Figs. 8 and 9 were constructed. The following paragraph describes how they were assigned to particular Pr isotopes. The level spins were assigned from a comparison with theoretical calculations, as described later in Sec. III.

Isotopic identification of the new cascades has been performed using the mass-correlation technique for complementary fission fragments proposed by Hotchkis *et al.* [12]. This method allows the mass of a fission fragment to be determined from the mean mass of its complementary partners. The mass distribution of the complementary fragments is obtained from their measured γ-ray intensities when gating on the fragment of interest. This technique has been used in many of our previous fission-fragment studies. A mass-correlation plot of mean rubidium-isotope mass, <A(Rb)>, versus praseodymium

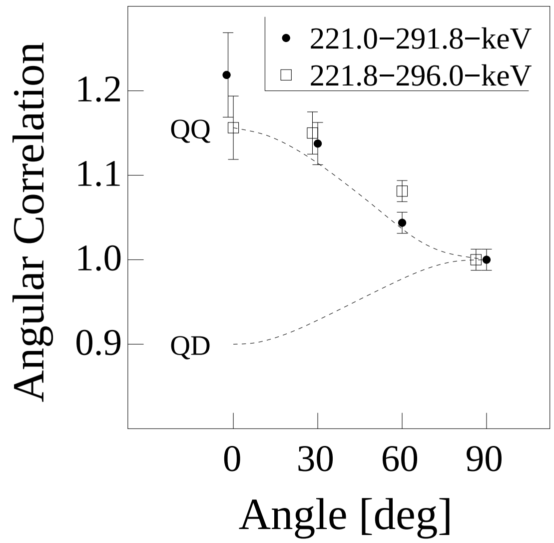

FIG. 7. Angular correlation measurements of γ rays in the new cascades. The lines show the theoretical values of $E2$–$E2$ (QQ) and $E2$–$E1$ (QD) correlations.

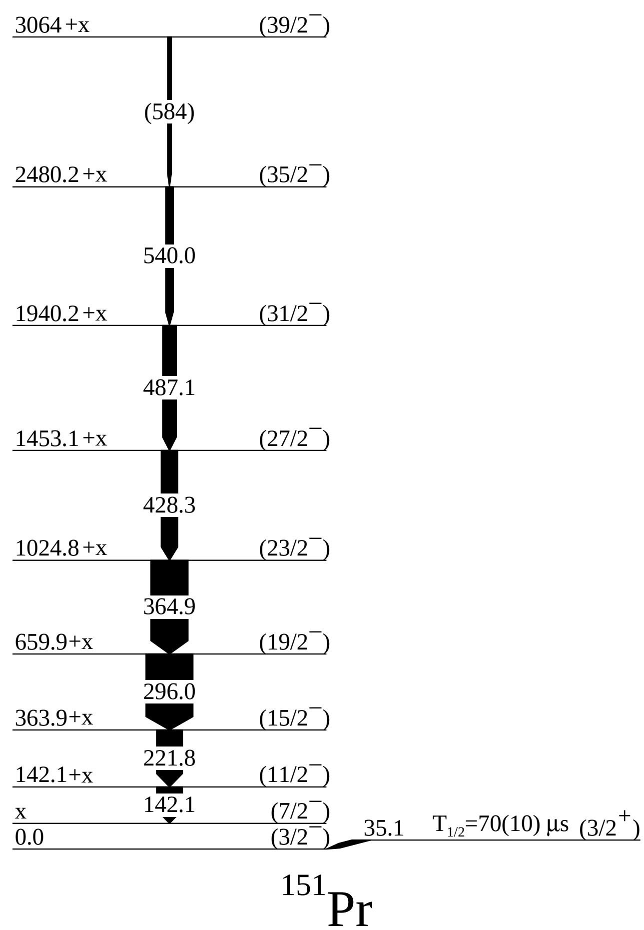

FIG. 8. Level scheme of ^{151}Pr, as obtained in this work.

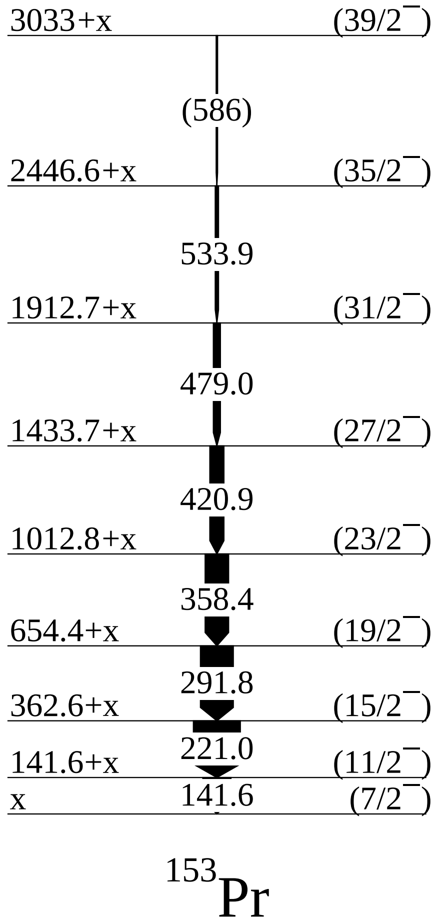

FIG. 9. Level scheme of ^{153}Pr, as obtained in this work.

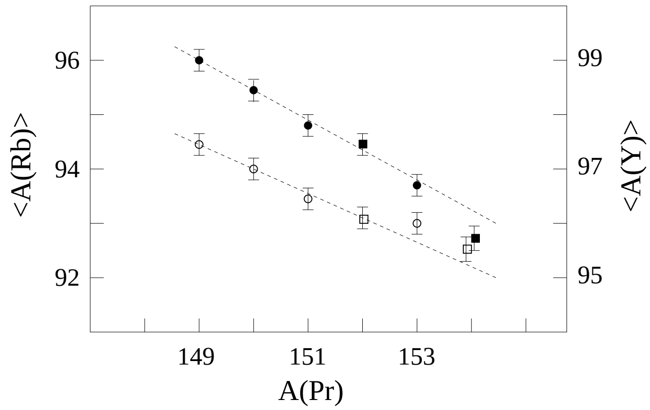

FIG. 10. Mass correlation plot for odd-A Pr isotopes, as obtained in this work from the ^{248}Cm fission data (empty circles and empty squares) and from ^{252}Cf fission data (full circles and full squares). Open and filled squares represent the average mass of Rb and Y isotopes obtained by gating on cascades assigned in Ref. [8] to ^{151}Pr and ^{153}Pr. These cascades are reassigned in this work to ^{152}Pr and ^{154}Pr, respectively. See the text for further explanations.

isotope mass, A(Pr), is shown in Fig. 10. The ^{248}Cm spontaneous-fission data points are shown as empty circles, corresponding to cascades from praseodymium isotopes with firm or new mass assignments, and empty squares, for previously reported cascades whose masses have been changed in the present work, as explained later. The first four empty circles (counting from left to right on the A(Pr) scale) were obtained by gating on γ lines from ^{149}Pr [6], the yrast cascade initially reported in [14] as ^{149}Pr, but reassigned later to ^{150}Pr [8] and from the new cascades containing the 221.8-, 296.0-, 364.9- and 221.0-, 291.8-, 358.4-keV γ rays. Data from a measurement using a ^{252}Cf source are also shown as full symbols in Fig. 10 and these are described in more detail later.

A straight line drawn through points for ^{149}Pr and ^{150}Pr, which have robust mass assignments, can be used as a guide for further isotopic assignments. Using this line, the point for the cascade containing the 221.8-, 296.0- and 364.9-keV transitions correlates well with ^{151}Pr. The data point for the cascade containing the 221.0-, 291.8-, 358.4-keV γ rays seems to fit well with ^{152}Pr, though it is two standard deviations away from the line when assigned to ^{153}Pr. However, the similarity of the two cascades shown in Figs. 8 and 9 suggests that both cascades belong to odd-A isotopes. Therefore, this cascade is preliminarily assigned to ^{153}Pr and further evidence supporting this is given below.

C. Gammasphere measurement

To verify the γ-ray coincidences and mass assignments obtained above, data from a measurement of γ rays following the spontaneous fission of ^{252}Cf, performed using the Gammasphere array of escape-suppressed germanium detectors, have been analyzed (see Ref. [27] for more information on the experiment).

Figures 11 and 12 show coincidences are between the three lowest-lying observed γ rays of the new cascades and confirm the decay schemes presented in Figs. 8 and 9. It is worth noting the visible difference in energy of the 221.0- and 221.8-keV transitions in Fig. 12. This will be referred to in Sec. IV. Table I shows the energies and intensities of the γ rays measured following the fission of ^{252}Cf and ^{248}Cm, reported above. Intensities are not reported for the 142.1- and 141.6-keV doublet as they could not be obtained reliably.

These data from the fission of ^{252}Cf also allowed a mass-correlation measurement to be performed between praseodymium isotopes and their complementary yttrium fragments, in an analogous way to that made above from the ^{248}Cm data set. The average masses of yttrium, <A(Y)>, nuclei observed in coincidence with γ decays from various Pr isotopes are shown as full circles in Fig. 10. Again, the <A(Y)> points, obtained by gating on γ lines in ^{149}Pr and ^{150}Pr, can serve as a calibration for the heavier Pr isotopes. The <A(Y)> observed in coincidence with the cascades containing the 221.8-, 296.0-, 364.9- and the 221.0-, 291.8-, 358.4-keV γ rays,

TABLE I. Energies and intensities of γ-ray transitions in ^{151}Pr and ^{153}Pr, following the spontaneous fission of ^{248}Cm and ^{252}Cf, as measured in the current work .

E_γ (keV)	I_γ (^{248}Cm) (rel. units)	I_γ (^{252}Cf) (rel. units)
	^{151}Pr	
142.1 (2)		
221.8 (2)	55(25)	
296.0 (2)	100(20)	100(10)
364.9 (2)	79(8)	67(7)
428.3 (2)	35(4)	44(5)
487.1 (2)	29(4)	30(4)
540.0 (3)	16(3)	11(3)
584 (1)	8(4)	
	^{153}Pr	
141.6 (2)		
221.0 (2)	70(30)	
291.8 (2)	100(10)	100(10)
358.4 (2)	105(10)	110(15)
420.9 (2)	67(7)	85(9)
479.0 (2)	27(4)	30(4)
533.9 (3)	14(3)	18(4)
586 (1)	8(4)	

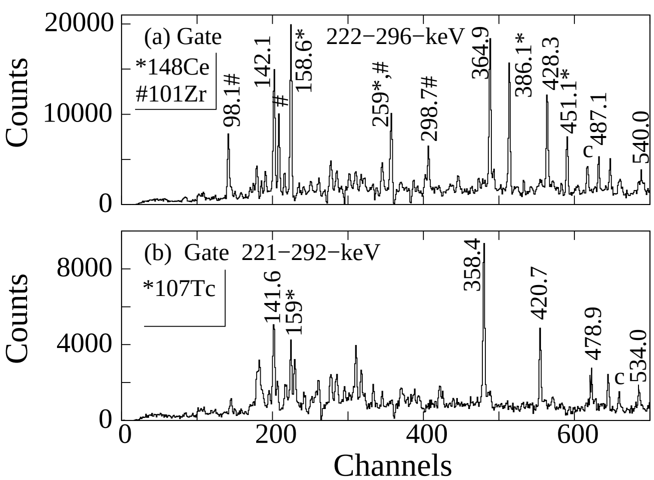

FIG. 11. Two γ-ray spectra obtained from the ^{252}Cf data set by double-gating on a) the 221.8- and 296.0-keV lines and b) the 221.0- and 291.8-keV lines of the new cascades.

fits well the calibration line, when assigned to ^{151}Pr and ^{153}Pr, respectively.

In order to increase the confidence in the isotopic assignments of the new γ-ray cascades, their intensities have been examined. This can give an independent verification of the mass assignments reported above. Figure 13(a) shows the intensity of triple-γ coincidences from the yrast cascades of ^{149}Pr and from those assigned to ^{151}Pr and ^{153}Pr in the present work. These intensities, which were corrected for detector efficiency and for in-

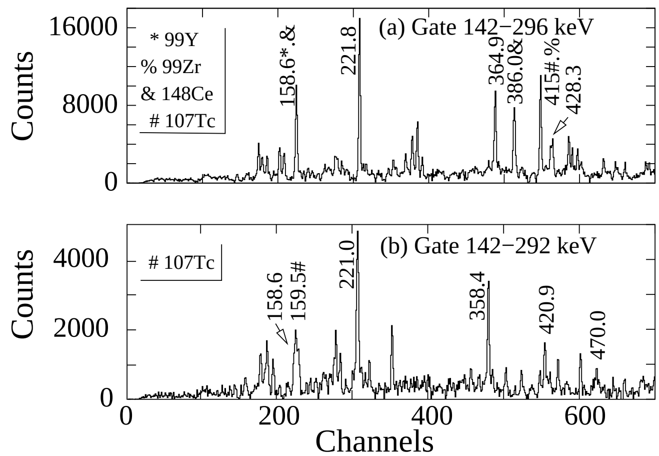

FIG. 12. wo γ-ray spectra obtained from the ^{252}Cf data set by double-gating on a) the 142.1- and 296.0-keV lines and b) the 141.6- and 291.8-keV lines of the new cascades

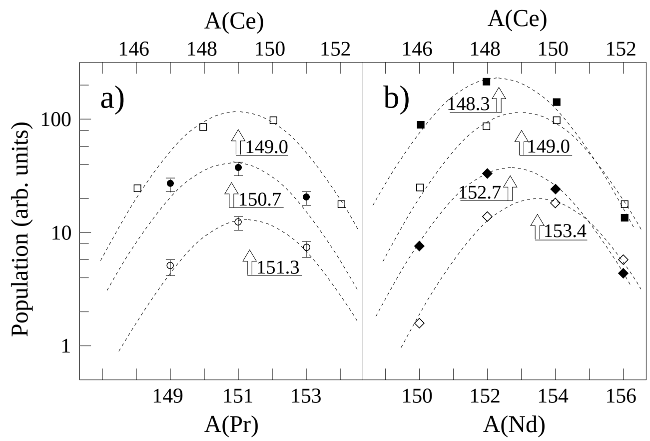

FIG. 13. Mass population diagrams for a) odd-A Pr and even-A Ce isotopes and b) for even-A Ce and Nd isotopes from the ^{248}Cm (empty symbols) and ^{252}Cf fission data (full symbols). Cerium, praseodymium, and neodymium isotopes are shown as circles, squares and diamonds, respectively. See text for further explanation.

ternal conversion-electron emission (assuming all transitions in the cascades are $E2$ in nature), are proportional to the production yields of the fission fragments. The full circles show the population of Pr isotopes following the fission of ^{252}Cf while the empty circles correspond to data from the fission of ^{248}Cm. The square symbols in Fig. 13 show the production of Ce isotopes following the fission of ^{248}Cm (empty) and ^{252}Cf (full), which are derived here from triple-γ coincidence intensities for the $6^+ \rightarrow 4^+ \rightarrow 2^+ \rightarrow 0^+$ cascades of the nuclei ^{146,148,150,152}Ce, where the error bars here are smaller than the symbol size. Analogous plots for the isotopes ^{150,152,154,156}Nd are shown in Fig. 13(b) for both ^{248}Cm (empty diamonds) and ^{252}Cf (full diamonds).

These cerium and neodymium data points were fitted by a Gaussian distribution which is shown as a dashed line,

$$P(A) = \frac{S}{\sqrt{2\pi\sigma^2}}\, e^{[-\frac{(A-A_0)^2}{2\sigma^2}]} \quad (1)$$

which describes well the production of fission fragments (see, for instance, the production of the neighboring barium isotopes in Ref. [4]). In the above formula A denotes mass number, while A_0, the centroid, and S, a parameter proportional to the amplitude, are left free in the fit. The width of the distribution, σ, was fixed to be 1.7, which comes from the systematic trends [28]. The S parameter will not be discussed, as the population is in arbitrary units. The centroid, $A_0(Ce)$, corresponding to the maximum population of the cerium isotopes following the spontaneous fission of ^{248}Cm, was found to be 149.0(1), from the data shown in Fig. 13. Similarly, a value of $A_0(Nd) = 153.4(1)$ was found for Nd isotopes and a value of $A_0(Ba) = 144.1$ was earlier reported for an analogous fit to barium isotopes from the same fissioning system [4]. The difference between these centroid positions allows one to estimate that $\Delta A_0 \sim 2.3$ per $\Delta Z = 1$ for heavy fission fragments, which can be used to verify the mass assignments of an isotopic chain.

Fitting the Pr data points from the ^{248}Cm data set of Fig. 13 with Equation 1 gives a centroid position of $A_0(Pr) = 151.3(1)$, in agreement with the value expected from the Ba, Ce and Nd data fits (151.3), giving an additional verification of the mass assignments for ^{149,151,153}Pr.

The ^{252}Cf data set was also used to extract this centroid for the Pr isotopes with the result $A_0(Pr) = 150.7(1)$. This is lower by 0.6(1) mass units than the centroid obtained from the ^{248}Cm data, in agreement with existing experimental data reporting more neutrons are evaporated, on average, in the fission of ^{252}Cf, $\bar{\nu} = 3.7(2)$ [29], than in the fission of ^{248}Cm, $\bar{\nu} = 3.5(5)$ [30].

The mean masses, A_0, extracted for each isotopic chain in the present work can also be compared to those obtained from the yields of spontaneous fission fragments in evaluated databases. These yields are evaluated for the ground states and long-lived isomeric states of fission fragments and so cannot be compared directly to the triple γ-ray coincidence data of the present study, which examines these nuclei at intermediate spins. Nuclei examined at different spins may have different mean neutron evaporation values, which therefore changes the mean mass of an isotopic chain. The relative differences between the mean masses of the different isotopic chains should however be similar for each type of study. For the fission of ^{248}Cm mean-mass differences of $\Delta A_0(Pr - Ce) = 2.34(7)$ and $\Delta A_0(Nd - Pr) = 2.08(9)$ respectively were extracted for the ground-states of isotopes from an evaluated database [31]. These compare well to the values of $\Delta A_0(Pr - Ce) = 2.3(1)$ and $\Delta A_0(Nd - Pr) = 2.2(1)$ measured in the present work with the ^{248}Cm data. The mean mass differences of $\Delta A_0(Pr - Ce) = 2.43(14)$ and $\Delta A_0(Nd - Pr) = 1.92(14)$ from the fission of ^{252}Cf were also obtained from an evaluated database [22]. Again, these compare well to the values of $\Delta A_0(Pr - Ce) = 2.4(1)$ and $\Delta A_0(Nd - Pr) = 2.0(1)$ measured in the current work from the fission of ^{252}Cf.

Finally, we have calculated average masses of Rb and Y isotopes, based on intensities of γ lines from these isotopes, as seen in the spectra gated on cascades assigned to ^{151}Pr and ^{153}Pr in Ref. [8]. The corresponding data are shown in Fig. 10 as open squares (for the ^{248}Cm data set) and filled squares (^{252}Cf fission data set). These data indicate that the cascade containing the 206.6-, 279.5-, and 351.1-keV transitions assigned in Ref. [8] to ^{153}Pr, actually belongs to a heavier Pr nucleus. We have assigned this cascade to ^{154}Pr, as shown in Fig. 10. Similarly, the cascade containing the 216.3-, 292.0-, and 363.3-keV γ rays, assigned in Ref. [8] to ^{151}Pr, is reassigned to ^{152}Pr from Fig. 10.

III. QUASI-PARTICLE-ROTOR MODEL CALCULATIONS AND STATE INTERPRETATIONS

The experimental data have been interpreted with the aid of Quasi-Particle-Rotor Model (QPRM) calculations, which were performed using the codes GAMPN, ASYRMO and PROBAMO [32]. Quasi-particle excitation energies, intraband transition energies and intraband transition probabilities were calculated. The programs use a modified-oscillator potential and diagonalize the particle-plus-triaxial-rotor Hamiltonian in the strong-coupling basis, with the single-particle matrix elements expressed in the deformed scheme, as described in [33]. Standard empirical values for the κ and μ strength parameters of the $l.s$ and l^2 terms have been used [34]. Input parameters to the model are A, Z and the deformations ϵ_2, ϵ_4, ϵ_6 and γ. The average Harris parameters, $\jmath_0$ and $\jmath_1$, of the neighboring even-even nuclei, at a spin of $\sim$8 $\hbar$, were used to calculate the variable moment of inertia. As the moment of inertia, $\jmath$, of the even-even cores was found to be non-linear at low spins, when plotted as a function of the squared frequency, then discrepancies will occur here between the predicted and observed intraband transition energies. Pairing correlations were included, via a standard BCS approximation, using values of $G_0 = 19.2$ MeV and $G_1 = 7.4$ MeV. Agreement between the experimental level energies and the theoretically predicted ones was improved for the negative-parity states by using an *ad hoc* "Coriolis attenuation" parameter of 0.7. This is a typical value for this parameter. No Coriolis attenuation was necessary for the positive-parity states. In order to calculate the $M1$ transition strengths a collective g-factor value for the core of $g_R = Z/A$ and an effective value of the free neutron g factor, $g_s^{eff} = 0.7 g_s^{free}$, were used.

A. QPRM Calculations and Interpretation of States of ^{151}Pr

Deformations of $\epsilon_2 = 0.26$ and $\epsilon_4 = -0.05$ have been used to calculate the levels of ^{151}Pr. The value of ϵ_2 was extracted from lifetime measurements of members of the ground-state band of the neighboring $N = 92$ isotone ^{152}Nd [35, 36], which translated to an average quadrupole moment of $Q_0 = 6.0(1)$ eb. In our recent work on the neighboring $N = 93$ nuclei ^{151}Ce, ^{153}Nd and ^{155}Sm [18] a hexadecapole deformation of $\epsilon_4 \sim -0.05$ was found to reproduce the decay schemes well. A comparison of the experimental and theoretical partial decay schemes is shown in Fig. 14, where the total decay intensity from each states is equal. Only decays of the favored-signature states are shown in this figure as these are expected to be considerably more intense than those of the unfavored states, as explained below. The lowest-lying positive- and negative-parity levels have both been set to an energy of 0 keV.

The nucleus ^{151}Pr has previously been assigned a ground-state spin and parity of $(3/2^-)$, from β-decay studies [37]. The calculations predict that the lowest-lying negative-parity state has a spin of $3/2^-$, with a strong $\pi 3/2^-[541]$ component. The 35.1-keV, 50-μs isomeric state decays by an $E1$ transition therefore it must originate from a positive-parity state with a possible spin of 1/2, 3/2 or 5/2. The calculations predict that the two lowest-lying positive-parity states, shown in Fig. 14, are nearly degenerate in energy and have strong components of the $1/2^+[420]$, $3/2^+[422]$ Nilsson orbitals. Other quasi-particle excitations are considerably higher in energy. If these two states are placed at 35.1 keV, and each one assumed to be the lowest-lying positive-parity state, then half-lives of 23 ns and 0.74 μs are predicted for the $1/2^+[420]$ and $3/2^+[422]$ bandhead states respectively, when corrected for internal conversion. Other spin 3/2 and 5/2 members of these bands are predicted to decay predominantly by intraband transitions with half-lives of a few ns. Although it is tempting to assign the isomeric state to have a dominant $3/2^+[422]$ configuration, from a comparison with the calculated half life, a $1/2^+[420]$ assignment cannot be completely ruled out. This is because the QPRM calculations cannot always reliably predict $E1$ transition rates, as shown in our recent works on ^{149}Pr [7] and ^{153}Nd [18], where the differences between the predicted and measured partial half lives were several orders of magnitude for one $E1$ transition in each nucleus.

The band on top of the $3/2^-[541]$ ground state is predicted to be yrast. As spontaneous fission is known to populate mostly yrast states, then the new γ-ray cascade of ^{151}Pr is assigned to the favored-signature members of the $3/2^-[541]$ band. The $7/2^- \rightarrow 3/2^-$ transition is calculated to be low in energy (20 keV), strongly converted and therefore would be unobserved in the spontaneous-fission data. A spin of $(7/2^-)$ can therefore be assigned to the state at the bottom of the new γ-ray cascade of ^{151}Pr. The calculations predict that the unfavored-signature members of this band are higher in energy than their counterpart $I + 1$ favored-signature states. This means that the favored states are predicted to decay only by stretched $E2$ transitions, in agreement with the observed decay pattern of the new cascade. No $E1$ decays are energetically possible from the favored-signature members of the $\pi 3/2^-[541]$ band.

The unfavored-signature states of the $3/2^-[541]$ band are predicted to decay with approximately half their population feeding lower lying $I - 2$ unfavored states, via stretched $E2$ transitions, and the other half of the population going to the favored-signature members of the same band. This means that the excited-state population will quickly accumulate in the favored-signature members of this band, confirming the decay pattern shown in Fig. 8. The unfavored members of the $3/2^-[541]$ band should be therefore the more difficult of the two signatures to observe. The intensity of decays from the unfavored negative-parity states to positive-parity ones, which are only possible above spin $13/2^-$, are calculated to be negligible.

Above spin $7/2^+$ the lowest-lying positive-parity states are calculated to be typically 100 keV, or more, higher in energy than the members of the $3/2^-[541]$ ground-state band with the same spin. As these states are non-yrast they will be more weakly populated than negative-parity states of the same spin, which may explain their non-observation in the present work. Favored members of bands based on the $1/2^+[420]$ and $3/2^+[422]$ states are predicted to be the most yrast positive-parity states, decaying predominantly by intraband $E2$ transitions without any strong $E1$ transitions feeding the $3/2^-[541]$ band, in agreement with our experimental observations from the prompt-fission data. About half the intensity of the decay of unfavored members of the $3/2^+[422]$ band decay feeds the $I - 1$ favored members of the same band, with the other half feeding the $I - 2$ unfavored members and just a few percent of the total decay intensity feeding the favored members of the $1/2^+[420]$ band. The unfavored members of the $1/2^+[420]$ decay with about half of their population feeding the $I - 2$ unfavored members of the same band and the rest of the intensity flowing almost equally to the favored and unfavored members of the $3/2^+[422]$ band. These predictions are in agreement with the high isomeric ratio observed for the 35.1-keV state, 19(12) %, which will collect the majority of the population of its band.

B. QPRM calculations and interpretation of states of ^{153}Pr

The nucleus ^{153}Pr has been calculated using identical parameters to those reported above used to calculate ^{151}Pr, with the exception of the moment of inertia parameters, which were obtained from the average $\jmath_0$ and $\jmath_1$ values of the neighboring even-even nuclei ^{152}Ce and

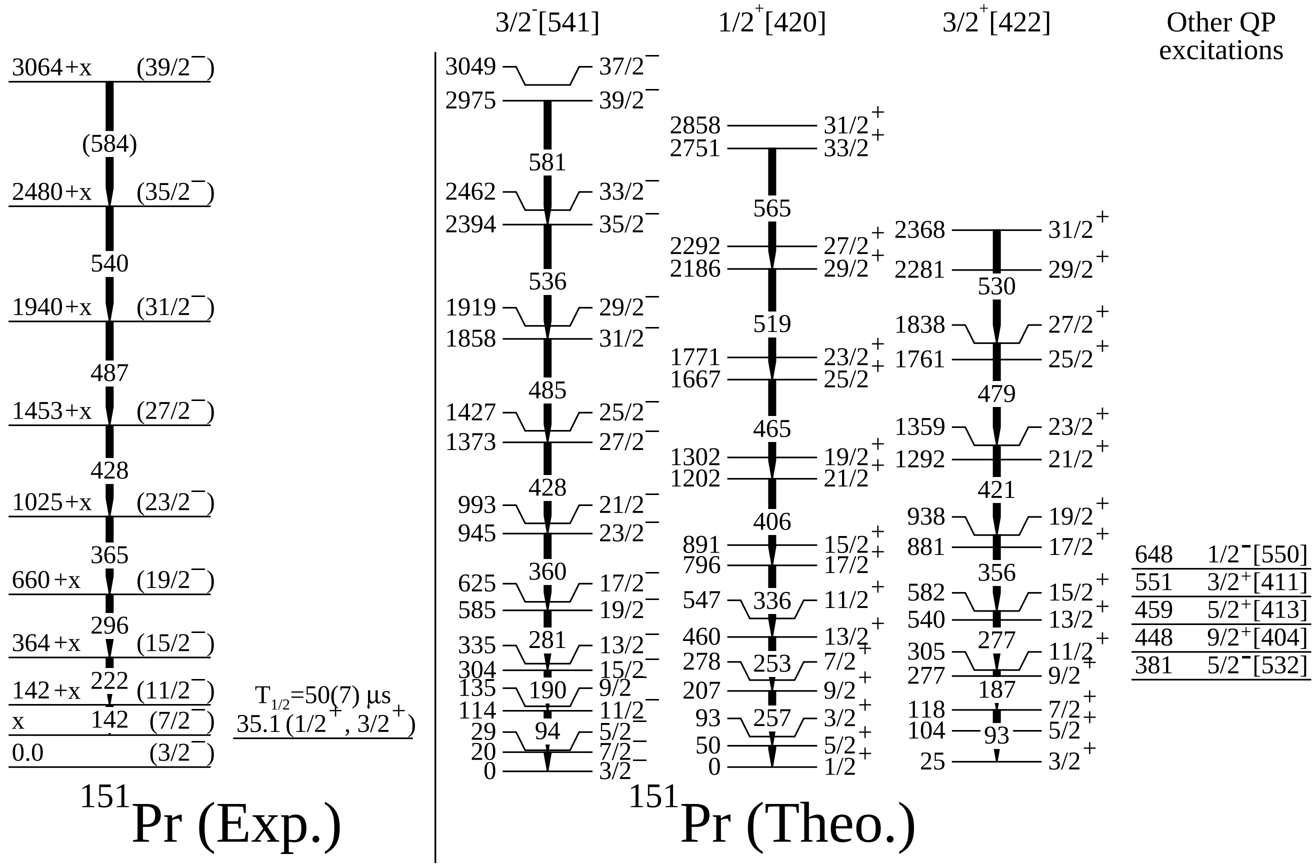

FIG. 14. Comparison of experimentally measured and calculated partial decay schemes of ^{151}Pr. See text for more details.

^{154}Nd. The quadrupole moments of intermediate-spin states of the ground-state bands of ^{152,154}Nd, extracted from lifetime measurements, have been found to be the same, within experimental errors [35]. As the quadrupole moment of ^{152}Nd was used to determine the deformation ϵ_2=0.26 for its $N = 92$ isotone ^{151}Pr, then the same value can be used to calculate ^{153}Pr. The calculated and experimental level schemes of ^{153}Pr are shown in Fig. 15, where all states are assumed to decay with the same total intensity. Here it can be seen that the energies and positions of the levels of ^{153}Pr are almost identical to those of ^{151}Pr, in agreement with the experimental observations.

The quasi-particle excitation energies and decay patterns of the excited states of ^{153}Pr are very similar to those described above for ^{151}Pr for both parities. The $3/2^-$[541] ground-state band is the most yrast of any parity and its favored members decay solely by stretched $E2$ γ rays. The unfavored members of this band decay to other states in this band with about half of their population feeding $I-2$ unfavored states and the remaining intensity decaying to $I-1$ favored band members. The yrast positive-parity states are again the favored members of the $1/2^+$[420] and $3/2^+$[422] bands. These favored states decay predominantly by stretched $E2$ transitions to other favored members of their band. The positive-parity states again lie higher in energy then the negative-parity states with the same spin, making them more difficult to observe as they will be more weakly populated in fission.

The $3/2^+$[422] quasi-particle excitation is again expected to have a μs isomeric character. In our recent examination of the neutron-rich $A = 153$ isotopes [18] we did not observe this predicted isomeric decay. The evaluated fission yield of ^{153}Pr, from neutron capture on ^{242}Am, is $6.3(27) \times 10^{-2}$ % [22], which is about a factor of 5 lower than that for ^{151}Pr with the same target ($3.2(8) \times 10^{-1}$ % [22]), though taking into account the large error, this may be as much as an order of magnitude. This lower production rate, combined with the strong isomeric decay of the 191.7-keV, 1.17-μs isomer of ^{153}Nd appearing in the same spectrometer setting, makes this predicted isomeric decay more difficult to observe than the one of ^{151}Pr.

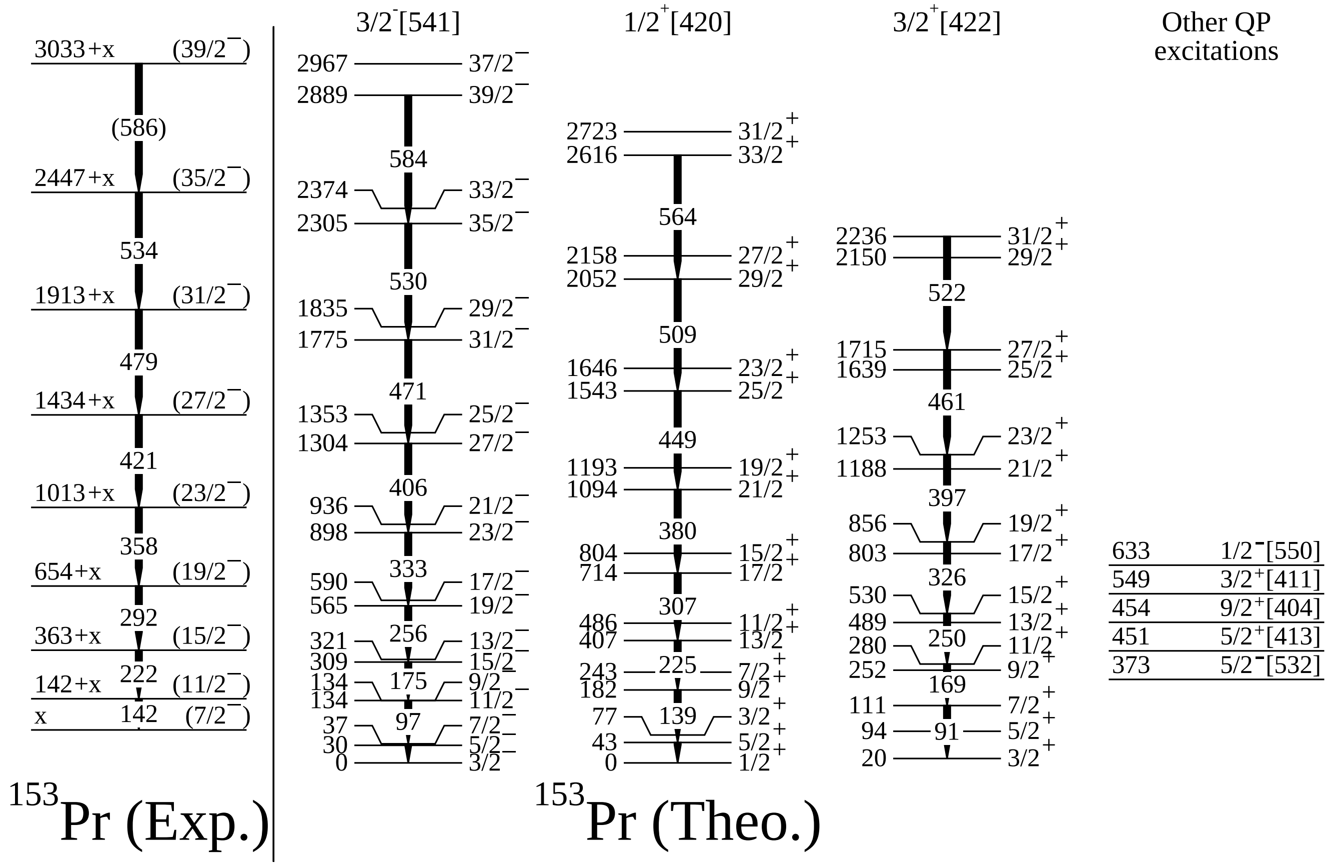

FIG. 15. Comparison of experimentally measured and calculated partial decay scheme of ^{153}Pr

C. Comparison of QPRM Calculations to Existing β-decay Data on ^{151}Pr

The new experimental data on ^{151}Pr and the QPRM calculations of the present work also allow the β-decay data reported in Ref. [20] concerning ^{151}Pr to be re-examined. The 35.1-keV isomeric state was previously assigned a spin and parity of ($7/2^+$) from lifetime arguments. However, this reasoning is weak as only a half-life limit of >10 μs could be assigned to this state in [20], leading to the assumption that the transition was $M2$ in nature. The conversion-coefficient measurement of the 35.1-keV transition reported above excludes this and a spin of ($1/2^+$, $3/2^+$) was assigned with the aid of the QPRM predictions.

Without more experimental information it is difficult to give firm spin assignments to any of the other excited states of ^{151}Pr reported at 38.9, 362.0, 402.6, 467.7 and 636.8 keV in [20], even with the aid of the QPRM calculations. Some useful observations may however be made. As the 362.0-, 402.6-, and 636.8-keV levels all feed both the $3/2^-$ ground state and the 38.9-keV state with similar intensities these last two states probably differ in spin by at most 1 $\hbar$. Therefore the 38.9-keV level has a spin and parity of either $1/2^+$, $3/2^+$ or $5/2^-$, from a comparison of states predicted by the QPRM calculations, shown in Fig. 14. It would be tempting to assign a negative parity to this state, and hence a spin of $5/2^-$, by assuming that the competing transitions feeding it and the ground state are $M1+E2$ in nature and knowing that the nearby 35.1-keV isomeric state has a low $B(E1)$ value. However $B(E1)$ values have been shown to differ by five orders of magnitude in the nearby nucleus ^{151}Pm [38] and competing $M1+E2$ and $E1$ decays which both feed the 38.9-keV state cannot be ruled out.

In the QPRM calculations a cluster of quasi-particle excitations appears at around 500 keV, containing the $5/2^-$[532], $9/2^+$[404], $5/2^+$[413], $3/2^+$[411], and $1/2^-$[550] orbitals. Recently the ground-state spin of ^{151}Ce was changed from ($5/2^+$) to ($3/2^-$) [18]. Members of the $9/2^+$[404] band are too high in spin to be populated directly from a β-decaying $3/2^-$ state. The 362.0-, 402.6-, 467.7-, and 636.8-keV states are therefore low-spin members of the other four bands. Comparisons between the predicted and experimental γ-decay branching ratios cannot give any firm assignments. Only the $3/2^-$[532] orbital and $3/2^-$ member of the $1/2^-$[550] band (predicted at 478 keV) give γ-decay $M1+E2$ branching ratios to the calculated $3/2^-$ and $5/2^-$ states with comparable intensities to those experimentally observed.

In Ref. [20] K X rays of Pr are reported to be in coincidence with themselves and the 38.9-, 40.6-, 142.1- and 323.1-keV γ rays. As the K electron binding energy of Pr is 41.99 keV then there must be other as-yet unobserved levels present in the β-decay scheme, as all γ transitions reported in [20] are either too low in energy (38.9, 40.6 keV) to be converted to K electrons, or too high in energy to be have high conversion coefficients (323.1 to 636.8 keV).

It is also worth noting that the $11/2^- \rightarrow 7/2^-$ decay observed in the prompt spontaneous-fission data reported in the present work, has the same energy as a 142.1-keV transition, which was unplaced in the β-decay scheme. The $11/2^-$ level may be indirectly populated following β decay. If these two transitions are the same, this gives independent confirmation of the assignment of the γ-ray cascade to ^{151}Pr.

IV. DISCUSSION

The levels of the bands of ^{151,153}Pr do not decay by any observed interband $E1$ decays and the 35.1-keV isomeric state of the nucleus ^{151}Pr has a low $B(E1)$ value of $6.3(10) \times 10^{-8}$ W.u. Therefore we can conclude that there is no evidence of any strong octupole collectivity in the states studied of ^{151,153}Pr. For the 35.1-keV isomeric transition of ^{151}Pr a dipole moment of $D_0 = 9.0(13) \times 10^{-4}$ $e.fm$ was extracted using the formula [39]

$$B(E1) = \frac{3}{4\pi} D_0^2 \langle I_i K_i 10 | I_f K_f \rangle^2. \tag{2}$$

This small dipole moment is in agreement with Hartree-Fock [40], cranked Woods-Saxon model calculations [41], and shell-corrected finite-range liquid drop model calculations [42] which all predict $\beta_3 = 0$ ($D_0 = 0$), for the ground states of ^{151}Pr or ^{150}Ce and ^{152}Nd, the immediate even-even neighbors of ^{151}Pr.

The results of the present work on ^{151,153}Pr are in agreement with our recent study of the deformed nuclei ^{153,154,156}Nd and ^{155,156,158,160}Sm [18, 19], where it was concluded that the isomeric one- or two-quasi-particle excitations are mostly responsible for the dipole moments of these states. Octupole correlations seem to be absent from these isomeric states. The absence of octupole correlations here can be related to increasing quadrupole deformation beyond $N = 90$. Quadrupole deformation is known to break the $(2j+1)$ degeneracy of spherical shell-model states and these states generally fan out in energy, with the energy splitting becoming larger with the increasing quadrupole deformation. The unique-parity orbitals follow undeviated trajectories, in a given harmonic oscillator shell, whereas natural-parity orbitals can be involved in orbital crossings which can further separate states with the same spherical shell-model state origin.

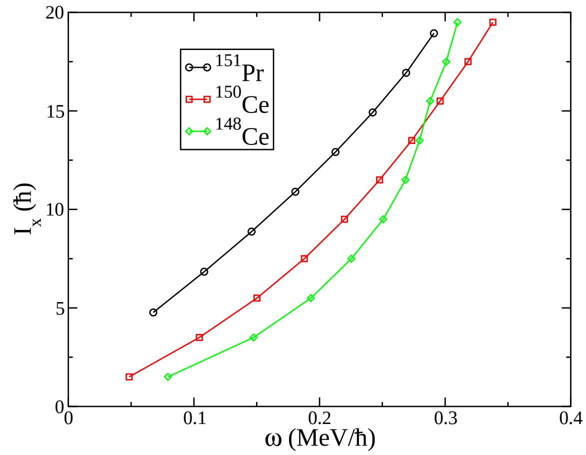

FIG. 16. (Color online) Aligned angular momentum of bands of ^{151}Pr and ^{148,150}Ce.

Simplistically, increasing quadrupole deformation should correspond to a general decrease in the strength of octupole collectivity. The situation is not so simple however as hexadecapole deformation is also present in the neutron-rich $A = 150$ region. This deformation multipole has the effect of quenching the energy splitting of the unique-parity Nilsson orbitals, as well as mixing $\Delta N = 2$ orbitals [43]. Theoretical calculations are required to better understand the experimental data obtained recently in this region.

The projections of the total aligned angular momentum on the rotation axis, I_x, of the $3/2^-[541]$ band of ^{151}Pr and the ground-state bands of ^{148,150}Ce [44] are shown in Fig. 16. At around 0.2 MeV/$\hbar$ the difference in I_x between the $3/2^-[541]$ band of ^{151}Pr and those of its Ce even-even neighbors is around 5 $\hbar$, in agreement with the proposed $\pi h_{11/2}$ origin of this band. The $3/2^-[541]$ band of ^{153}Pr is not shown in Fig. 16 as it has very similar energies to those of the band of ^{151}Pr. This is another case of bands with very similar transition energies, which are common in this region and have been reported for the Nd and Sm nuclei with $N > 92$ in [18, 19, 44] and references therein. Beyond 0.25 MeV/$\hbar$ evidence of an "upbend" is seen in Fig. 16 for ^{148}Ce, which is in agreement with calculations for the nearby samarium isotones [45]. These predict the first band crossing of ^{152}Sm, an isotone of ^{148}Ce, to be one involving the $\nu 3/2[651]$ orbital, at about 0.23 MeV/$\hbar$. For heavier samarium isotopes the first band crossings, which again involve orbits originating from the spherical $\nu i_{13/2}$ states, move to slightly higher frequencies ($\gtrsim$0.25 MeV/$\hbar$), though no evidence of any band-crossings for ^{150}Ce and ^{151}Pr are seen in Fig. 16.

During the course of this work two publications have appeared, one of them very recently, which assigned bands to ^{151,153}Pr [8] and ^{152}Pr [46]. The parity-doublet bands assigned to ^{151,153}Pr in Ref. [8] seem to be incorrect, not only from the experimental mass-assignment arguments put forward in Sec. II B, but also from a theoretical point of view. The negative-parity bands reported in [8] were said to be based on the $\pi 3/2^-[541]$ orbital, whose origin is the spherical $\pi h_{11/2}$ spherical state. The most intense decays of these bands should proceed through the favored-signature states, as predicted by the QPRM calculations presented in Sec. III. The bands assigned to ^{151,153}Pr in [8] however contain states with the spins $5/2^-$, $9/2^-$, $13/2^-$ which are unfavored and such a decay sequence is therefore unlikely. The slow $E1$ transition reported for the 35.1-keV isomer of ^{151}Pr in the present work also shows that decays between states with different parities may be strongly hindered. As mentioned above several microscopic calculations [40–42], predict $\beta_3 = 0$, for the ground states of ^{150}Ce and ^{152}Nd, the immediate even-even neighbors of ^{151}Pr, and no softness to octupole modes at higher spins in these nuclei [41]. The level scheme of ^{149}Pr does not show any hint of octupole collectivity [7] hence it would be unlikely that octupole modes develop in ^{151,153}Pr which are more deformed and further away from $N = 90$, where the maximum number of octupole-collectivity forming orbital lie close to the surface, at weak deformations. As mentioned in Sec. II B, we propose that these bands actually belong to the neighboring odd-odd Pr nuclei and more complete level schemes, including additional low-lying transitions, will be presented in a forthcoming article.

Very recently two bands were attributed to ^{152}Pr in [46] and the energies of the transitions in the two bands are almost identical to those assigned to ^{151,153}Pr in the present work, hence one can assume that these are the same cascades. Some differences in these cascades exist however. The cascade of the second band in ^{152}Pr decays into the second excited state of the first band, which decays by a 221.9-keV transition, followed by a 142.3-keV γ-ray to the bandhead of the first state. In the present work the lowest two observed transitions in the cascade of ^{151}Pr have energies of 141.1 and 221.8 keV. For ^{153}Pr these energies are 141.6 and 221.0 keV. The 0.5- and 0.8-keV energy differences between the centroids of the two lowest transitions in each cascade can be measured in γ-ray peaks with several thousand counts, as can be seen in Fig. 12. It is not explained which transitions are used to make the mass assignment of $A = 152$ in [46]. One notes that if all transitions are used, or just the two lowest, one ends up with an average of the two masses 151 and 153, which is 152. The transition energies of these two bands assigned to ^{152}Pr are very similar to each other and it would be unusual to find such bands in the same odd-odd nucleus. On the other hand, as mentioned above, and in Ref. [19], bands with almost identical transition energies are common in neighboring nuclei in this region.

V. CONCLUSION

New rotational bands have been reported and assigned to ^{151,153}Pr from a careful analysis of two sets of spontaneous fission data. A delayed 35.1-keV, previously assigned to ^{151}Pr, has been determined to be $E1$ in multipolarity, from conversion-electron measurements and a half life of 50(8) μs was determined for this transition, for the first time. The assignment of this isomer to ^{151}Pr has been verified using the measured isomeric population and evaluated fission yields. Calculations presented here using a QPRM are able to reproduce the decay sequence of these bands and allow the ground state bands to be assigned a $3/2^-[541]$ configuration and the isomeric state a $3/2^+[422]$ or $1/2^+[420]$ configuration. The slow $E1$ isomeric transition and the non-observation of interband $E1$ transitions for ^{151,153}Pr show an absence of strong octupole correlations in these nuclei. These results are in agreement with our recent measurements on Nd and Sm nuclei with $N > 92$, where again no evidence of octupole correlations was observed in the states observed [18, 19]. A phenomenological examination of the Nilsson orbits present here allow an explanation for this to be put forward in terms of an absence of octupole generating orbits, due to increasing quadrupole deformation and orbital crossings. These separate out the states required to form octupole correlations. These conclusions are in agreement with theoretical calculations which do not predict these nuclei to be octupole deformed [40–42] or to be soft to octupole modes [41] at higher spins.

ACKNOWLEDGMENTS

This work has been partly supported by the U.S. Department of Energy, Office of Nuclear Physics, under contract No. DE-AC02-06CH11357. The authors are grateful for the use of ^{248}Cm to the Office of Basic Energy Sciences, US Department of Energy, through the transplutonium element production facilities at the Oak Ridge National Laboratory. We would like to thank M. P. Carpenter, R. V. F. Janssens, F. G. Kondev, T. Lauritsen, C. J. Lister and D. Seweryniak of the Physics Division of Argonne National Laboratory for their help in preparing and running the Gammasphere. measurement.

[1] G. A. Leander, W. Nazarewicz, P. Olanders, I. Ragnarsson, and J. Dudek, Phys. Lett.**152B**, 284 (1985).

[2] W. R. Phillips, I. Ahmad, H. Emling, R. Holzmann, R. V. F. Janssens, T. L. Khoo, and M. W. Drigert, Phys. Rev. Lett.**57**, 3257 (1986).

[3] W. Urban, M. A. Jones, J. L. Durell, M. J. Leddy, W. R. Phillips, A. G. Smith, B. J. Varley, and I. Ahmad, Phys. Lett. **A613**, 107 (1997).

[4] W. Urban,M. A. Jones, J. L. Durell, M. J. Leddy, W. R. Phillips, A. G. Smith, B. J. Varley, I. Ahmad, L. R. Morss, M. Bentaleb, E. Lubkiewicz, and N. Schulz, Nucl. Phys. **A613**, 107 (1997).

[5] P. Kleinheinz, R. .K. Sheline, M. R. Maier, R. M. Diamond, and F. S. Stephens, Phys. Rev. Lett. **34**, 68 (1974).

[6] T. Rząca-Urban, W. Urban, J. A. Pinston, G. S. Simpson, J. L. Durell, A. G. Smith, and I. Ahmad, Phys. Rev. C **82**, 017301 (2010).

[7] T. Rząca-Urban, W. Urban, J. A. Pinston, G. S. Simpson, A. G. Smith, J. F. Smith, and I. Ahmad, Phys. Rev. C, **82**, 067304 (2010).

[8] J. K. Hwang, A. V. Ramayya, J. H. Hamilton, S. H. Liu, N. T. Brewer, Y. X. Luo, J. O. Rasmussen, S. J. Zhu, and R. Donangelo, Phys. Rev. C **82**, 034308 (2010).

[9] J. K. Hwang, A. V. Ramayya, J. H. Hamilton, S. H. Liu, N. T. Brewer, Y. X. Luo, J. O. Rasmussen, S. J. Zhu, and R. Donangelo, Phys. Rev. C **82**, 049901(E) (2010).

[10] I. Tsekhanovich, G. S. Simpson, W. Urban, J. A. Dare, J. Jolie, A. Linnemann, R. Orlandi, A. Scherillo, A. G. Smith, T. Soldner, B. J. Varley, T. Rząca-Urban, A. Złomaniec, O. Dorvaux, B. J. P. Gall, B .Roux, and J. F. Smith, Phys. Rev. C **78**, 011301(R) (2008).

[11] G. S. Simpson, W. Urban, K. Sieja, J. A. Dare, J. Jolie, A. Linneman, R. Orlandi, A. Scherillo, A. G. Smith, T. Soldner, I. Tsekhanovich, B. J. Varley, A. Złomaniec, J. L. Durell, J. F. Smith, T. Rząca-Urban, H. Faust, I. Ahmad, and J. P. Greene, Phys. Rev. C **82**, 024302 (2010).

[12] M. A. C Hotchkis, J. L. Durell, J. B Fitzgerald, A. S. Mowbray, W. R. Phillips, I. Ahmad, M. P. Carpenter, R. V. F. Janssens, T. L. Khoo, E. F. Moore, L. R. Morss, Ph. Benet, and D. Ye, Nucl. Phys. **A530**, 111 (1991).

[13] W. Urban, W. R. Phillips, N. Schulz, B. J. P. Gall, I. Ahmad, M. Bentaleb, J. L. Durell, M. A. Jones, M. J. Leddy, E. Lubkiewicz, L. R. Morss, A. G. Smith, and B. J. Varley, Phys. Rev. C **62**, 044315 (2000).

[14] J. K. Hwang, A. V. Ramayya, J. H. Hamilton, E. F. Jones, P. M. Gore, S. J. Zhu, C. J. Beyer, J. Kormicki, X. Q. Zhang, L. K. Peker, B. R. S. Babu, T. N. Ginter, *et al.*, Phys. Rev. C **62**, 044303 (2000).

[15] J. H. Hamilton, Y. X. Luo, J. K. Hwang, E. F. Jones, A. V. Ramayya, S. J. Zhu, P. M. Gore, C.J. Beyer, J. Kormicki, *et al.*, Acta Phys. Pol. **32**, 957 (2001).

[16] Y. X. Luo, Y. X. Luo, J. H. Hamilton, J. O. Rasmussenb, A. V. Ramayya, C. Goodin, S. J. Zhu, J. K. Hwang, K. Li, D. Fong, I. Stefanescu, I. Y. Lee, *et al.*, Nucl. Phys. **A818**, 121 (2009).

[17] J. K. Hwang, A. V. Ramayya, J. Gilat, J. H. Hamilton, L. K. Peker, J. O. Rasmussen, J. Kormicki, T. N. Ginter, *et al.*, Phys. Rev. C **58**, 3252 (1998).

[18] G. S. Simpson, W. Urban, J. A. Pinston, J. C. Angelique, I. Deloncle, H. R. Faust, J. Genevey, U. Köster, T. Materna, R. Orlandi, A. Scherillo, A. G. Smith, J. F. Smith, T. Rząca-Urban, I. Ahmad, and J. P. Greene, Phys. Rev. C **81**, 024313 (2010).

[19] G. S. Simpson, W. Urban, J. Genevey, R. Orlandi, J. A. Pinston, A. Scherillo, A. G. Smith, J. F. Smith, I. Ahmad, and J. P. Greene, Phys. Rev. C **80**, 024304 (2009).

[20] Y. Kojima, M. Shibata, A. Taniguchi, Y. Kawase, R. Doi, A. Nagao, and K. Shizuma, Nucl. Instrum. Methods **A 564**, 275 (2006).

[21] T. Kibédi, T. W. Burrows, M. B. Trzhaskovskaya, P. M. Davidson, and C. W. Nestor Jr., Nucl. Instrum. Methods A **589**, 202 (2008).

[22] JEFF3.1.1, Joint Evaluated Fission and Fusion (JEFF) project, an evaluated database of fission data maintained by the NEA. http://www.oecd-nea.org/dbdata/jeff/

[23] B. Singh, Nucl. Data Sheets **110**, 1 (2009).

[24] P. J. Nolan, F. A. Beck, and D. B. Fossan, Ann. Rev. Nuc. Part. Sci. 44, 561 (1994).

[25] W. Urban *et al.*, Eur. Phys. J. A **5**, 239 (1999).

[26] W. Urban *et al.*, Z. Phys. A **358**, 145 (1997).

[27] D. Patel, A. G. Smith, G. S. Simpson, R. M. Wall, J. F. Smith, O. J. Onakanmi, I. Ahmad, J. P. Greene, M. P. Carpenter, T. Lauritsen, C. J. Lister, R. V. F. Janssens, F. G. Kondev, D. Seweryniak, B. J. P. Gall, O. Dorveaux, and B. Roux, J. Phys. G. Nucl. Part. Phys. **28**. 649 (2002).

[28] A. C. Wahl, At. Data and Nucl. Data Tables **39**, 1 (1988).

[29] G. M. Ter-Akopian *et al.*, Phys. Rev. C **55**, 1146 (1997)

[30] K. F. Flynn, J. E. Gindler and L. E. Glendenin J. Inorg. and Nucl. Chem. **39** 759 (1977).

[31] ENDF/B-VII.1, Evaluated Nuclear Data File, an evaluated database of nuclear reaction data maintained by the CSEWG. http://www.nndc.bnl.gov/exfor/endf00.jsp

[32] P. Semmes and I. Ragnarsson, *The Particle plus Triaxial Model: a User's Guide* distributed at the Hands-on Nuclear Physics Workshop, Oak Ridge, 5-16 August 1991 (unpublished).

[33] S. E. Larsson, G. Leander, and I. Ragnarsson, Nucl. Phys. **A307**, 189 (1978).

[34] T. Bengtsson and I. Ragnarsson, Nucl. Phys. **A436**, 14 (1985).

[35] A. G. Smith, W. R. Phillips, J. L. Durell, W. Urban, B. J. Varley, C. J. Pearson, J. A. Shannon, I. Ahmad, C. J. Lister, L.R. Morss, *et al.*, Phys. Rev. Lett. **73**, 2540 (1994).

[36] M. Hellström, H. Mach, B. Fogelberg, D. Jerrestam, and L. Spanier, Phys. Rev. C **47**, 545 (1993).

[37] M. Shibata, T. Ikuta, A. Taniguchi, A. Osa, A. Tanaka, H. Yamamoto, K. Kawade, J.-Z. Ruan, Y. Kawase, and K.Okano, J. Phys. Soc. Jpn. **63**, 3263 (1994).

[38] W. Urban, J. C. Bacelar, W. Gast, G. Hebbinghaus, A. Kramer-Flecken, R. M. Lieder, T. Morek, and T. Rząca-Urban, Phys. Lett. **247B**, 238 (1990).

[39] P. A. Butler and W. Nazarewicz, Nucl. Phys. **A533**, 249 (1991).

[40] J. L. Egido and L. M. Robledo, Nucl. Phys. **A545**, 589 (1992).

[41] W. Nazarewicz and S. L. Tabor, Phys. Rev. C **45** 2226 (1992).

[42] P. Möller, J. R. Nix, W. D. Myers, and W. J. Swiatecki, At. Data Nucl. Data Tables **59**, 185 (1995).

[43] A. K. Jain, R. K. Sheline, P. .C. Sood, K. Jain Rev. Mod. Phys. **62**, 393 (1990).

[44] S. J. Zhu, *et al.*, J. Phys. G **21** L75 (1995).

[45] R. Bengtsson, S. Frauendorf, and F.-R. May, Atomic Data and Nuclear Data Tables **35**, 15 (1986).

[46] S. H. Liu, J. H. Hamilton, A. V. Ramayya, Y. Shi, F. R. Xu, S. J. Zhu, E. Y. Yeoh, J. C. Batchelder, N. T. Brewer, J. K. Hwang, Y. X. Luo, J. O. Rasmussen, W. C. Ma, A. V. Daniel, G. M. Ter-Akopian, and Yu. Ts. Oganessian, Phys. Rev. C **84**, 044303 (2011).